Sensors and Actuators: A. Physical 334 (2022) 113357

Contents lists available at ScienceDirect

Sensors and Actuators: A. Physical

journal homepage: www.elsevier.com/locate/sna

Effect of As flux on InAs submonolayer quantum dot formation for infrared photodetectors

A. Alzeidan[a,*], T.F. Cantalice[a], K.D. Vallejo[b], R.S.R. Gajjela[c], A.L. Hendriks[c], P.J. Simmonds[b,d], P.M. Koenraad[c], A.A. Quivy[a]

[a] Institute of Physics, University of Sao Paulo, Sao Paulo, SP 05508-090, Brazil
[b] Micron School of Materials Science and Engineering, Boise State University, Boise, ID, USA
[c] Department of Applied Physics, Eindhoven University of Technology, Eindhoven, AZ 5612, The Netherlands
[d] Department of Physics, Boise State University, Boise, ID, USA

ARTICLE INFO

Article history:
Received 3 October 2021
Received in revised form 9 December 2021
Accepted 28 December 2021
Available online 30 December 2021

Keywords:
Submonolayer quantum dots
Infrared photodetector
Segregation
InAs
Scanning tunneling microscopy
Molecular beam epitaxy

ABSTRACT

The performance of infrared photodetectors based on submonolayer quantum dots was investigated as a function of the arsenic flux. All the devices showed similar figures of merit and a very high specific detectivity above 1 × 10^{11} cm $Hz^{1/2}$/W at 12 K, despite the fact that cross-sectional scanning tunneling microscopy images pointed out a strong reduction in the density of such nanostructures with decreasing arsenic flux. This contrast is a consequence of the small size and low In content of the submonolayer quantum dots that lead to a strong delocalization of the electrons wave function and, therefore, reduce the advantage of samples having a very high density of quantum dots. A simple strain model showed that the properties of these nanostructures are limited by the lack of vertical alignment of the small two-dimensional InAs islands resulting from the strong segregation of In atoms. We have proposed some ways to improve the growth of submonolayer quantum dots and believe that, after further optimization, such nanostructures might provide devices with superior performance.

1. Introduction

In the last two decades, quantum-dot infrared photodetectors (QDIPs) have been the subject of active research. They utilize intersubband transitions between different electronic states of low-dimensional nanostructures, as is also the case in the more famous quantum-well infrared photodetectors (QWIPs). However, the three-dimensional (3D) carrier confinement provided by quantum dots (QDs) offers several advantages over QWIPs, including a lower dark current, normal-incidence detection, higher operating temperature, and higher detectivity [1–6]. In general, QDIPs are based on self-assembled InAs QDs deposited on a GaAs(001) substrate using the Stranski-Krastanov (SK) growth mode. Above a critical thickness of 1.7 monolayers (MLs), the thin InAs layer–that is under compressive strain due to the smaller lattice parameter of the GaAs material–spontaneously forms an ensemble of small and homogeneous 3D InAs islands that can confine the carriers in all three spatial dimensions, behaving thus as quantum dots. Such Stranski-Krastanov quantum dots (SK-QDs) are surrounded by a thin InGaAs wetting layer and usually have a lens or truncated-pyramid shape, a density in the low-to-mid 10^{10} cm^{-2} range, and a base and height on the order of 10–20 nm and 3–7 nm, respectively [7–11]. However, SK-QDs suffer from poor QD size control, a relatively low density and the presence of a wetting layer that introduces extra stress in the samples and reduces the 3D confinement of the carriers.

Submonolayer quantum dots (SML-QDs) have emerged as a possible solution to these problems with SK-QDs [12]. InAs/GaAs SML-QDs can be obtained by depositing a fraction of a monolayer of InAs material–generally between 0.3 and 0.5 ML to nucleate a very high density of small two-dimensional (2D) islands on the GaAs substrate–and then a few monolayers of GaAs. By repeating this sequence several times, one expects the small 2D islands in each InAs submonolayer to nucleate above those of the previous InAs submonolayer, as a consequence of the elastic strain present in the InAs/GaAs system. Therefore, vertical stacks of 2D InAs islands will be formed and will thus behave as individual quantum dots, leading to a very high density (up to 10^{12} cm^{-2}) of nanostructures with a particular height that can be obtained in a controllable way [13].

Until now, all the infrared photodetectors based on submonolayer quantum dots (SML-QDIPs) have been obtained using

* Corresponding author.
E-mail address: alzeidan@if.usp.br (A. Alzeidan).

https://doi.org/10.1016/j.sna.2021.113357
0924-4247/

growth parameters similar to those employed for SK-QDs. After growing the GaAs buffer, the substrate temperature is reduced while maintaining a high As flux, which results in the formation of a c(4×4) reconstruction of the GaAs(001) surface prior to InAs deposition. Although QDIPs fabricated with SML-QDs deposited in such conditions clearly show improved performance when compared to the same devices containing SK-QDs [14–17], it seems that SML-QDs grown in these conditions are probably not resulting from the vertical alignment of small 2D InAs islands. Indeed, scanning tunneling microscopy measurements showed that, when the InAs material is deposited on top of a c(4×4)-reconstructed GaAs(001) surface, the In atoms are actually randomly incorporated into the deep As trenches, yielding an InGaAs alloying of the surface [18], while true 2D InAs islands can only be nucleated in the presence of a (2×4) reconstruction of the GaAs(001) surface [19].

Since, for a fixed sample temperature, the surface reconstruction is a function of the As flux, in this paper we investigated the influence of the As flux on the properties of SML-QDs and analyzed the results on the basis of cross-sectional scanning tunneling microscopy (X-STM) and device-performance data.

2. Experimental details

All the QDIPs analyzed here had exactly the same structure–they only differed by the As flux during formation of the SML-QDs–and were grown by molecular beam epitaxy (MBE) on top of an epi-ready undoped GaAs(001) substrate. They consisted of two 1 μm-thick Si-doped GaAs layers (doping concentration n = 1 × 10^{18} cm^{-3}) grown at 570 °C acting as bottom and top contacts. In between them, the active region was formed by ten GaAs quantum wells (QWs), each surrounded by 45 nm wide $Al_{0.1}Ga_{0.9}As$ barriers deposited at 580 °C. The inner part of each well was grown at 490 °C and started with 1.3 nm of GaAs followed by the SML-QDs, composed of six repetitions of a basic cycle formed by 0.5 ML of InAs and 2.5 MLs of GaAs, which were covered by 2.1 nm of GaAs (Fig. 1). Each 2.5 ML-thick GaAs spacer was Si doped at 2 × 10^{18} cm^{-3} to provide the doping of the SML-QDs.

To minimize In desorption from the surface, deposition of InAs has to occur at low temperature, generally below 515 °C. These typical growth conditions employed to obtain SK-QDs systematically lead to a c(4×4) reconstruction of the GaAs(001) surface due to the high As flux (equivalent to 1–2 ML/s). To maintain a (2×4) reconstruction as the sample is cooled after growing the AlGaAs barriers, the As flux has to be considerably reduced [20]. For the sample temperature used in the present work (490 °C), the transition between both reconstructions was observed for an As flux around 0.2 ML/s on the fluorescent screen of the reflection high-energy electron diffraction (RHEED) system [21]. Therefore, three SML-QDIPs having exactly the same structure were grown, the only difference among them being the As_2 flux–coming from a valved cracker–that was set to 0.15 ML/s, 0.25 ML/s, and 1.90 ML/s for SML-QDIP A, B, and C, respectively. Sample A was grown with a (2×4) surface reconstruction prior to InAs deposition, sample B was grown with a slightly higher As flux and a c(4×4) reconstruction (just above the (2×4) to c(4×4) transition), and sample C was also grown with a c (4×4) reconstruction but with the much higher As flux generally used for SK-QDs. Since the As flux necessary to reach the (2×4) reconstruction was extremely low, the growth rates of the GaAs and InAs materials used for the SML-QDs also had to be considerably reduced and were set to 0.1 ML/s and 0.015 ML/s, respectively. These three samples allowed us to simultaneously check the importance of the surface reconstruction (comparing samples A and B which have a similar As flux) and to investigate the possible influence of a large variation of the As flux (comparing samples B and C which have the same surface reconstruction). Additionally, sample C served as a reference as it was grown in conditions close to the ones of SK-QDs,

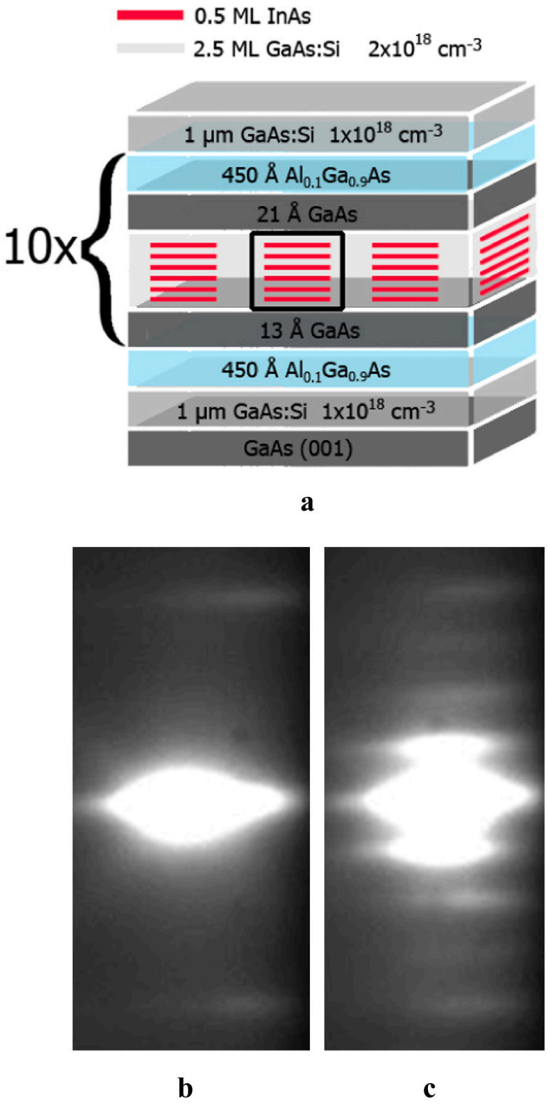

Fig. 1. a) Structure of SML-QDIPs A, B, and C. The black rectangle shows a single SML-QD formed by repeating six times the deposition of 0.5 ML of InAs followed by 2.5 MLs of GaAs:Si. The only difference between the 3 samples was the arsenic flux used to grow the SML-QDs of each device. b) RHEED pattern of the (2×4) GaAs(001) surface using an As flux of 0.15 ML/s. c) RHEED pattern of the c(4×4) GaAs(001) surface obtained with an As flux of 0.25 ML/s and 1.90 ML/s. Both patterns were obtained along the [010] azimuth.

as usually done in the literature. The three samples were processed into 400 × 400 μm^2 mesas using optical lithography, wet etching, metal deposition (Ni/Ge/Au, 25/55/150 nm) and rapid thermal annealing at 520 °C for 30 s to get good Ohmic contacts. The devices were wire bonded to the pads of a chip carrier that was plugged into the cold finger of a closed-loop He cryostat having a Ge window and operating between 10 and 300 K.

A last sample, that will be called sample D, was specifically grown on a Si-doped GaAs(001) substrate (n = 1 × 10^{18} cm^{-3}) to allow X-STM measurements and contained SML-QDs layers A1, B1, and C1 that were deposited with the same growth parameters as the SML-QDs of samples A, B, and C, respectively. The only differences are that, in sample D, the SML-QDs layers were separated from each other by 200 nm of GaAs, and the 2.5 ML-thick GaAs spacers were undoped to avoid any influence of the Si dopant on the topographic measurements. The sample was cleaved under ultra-high vacuum and measured by STM at 77 K on a freshly obtained {110} surface. More information about this sample and previous X-STM measurements can be found in [22].

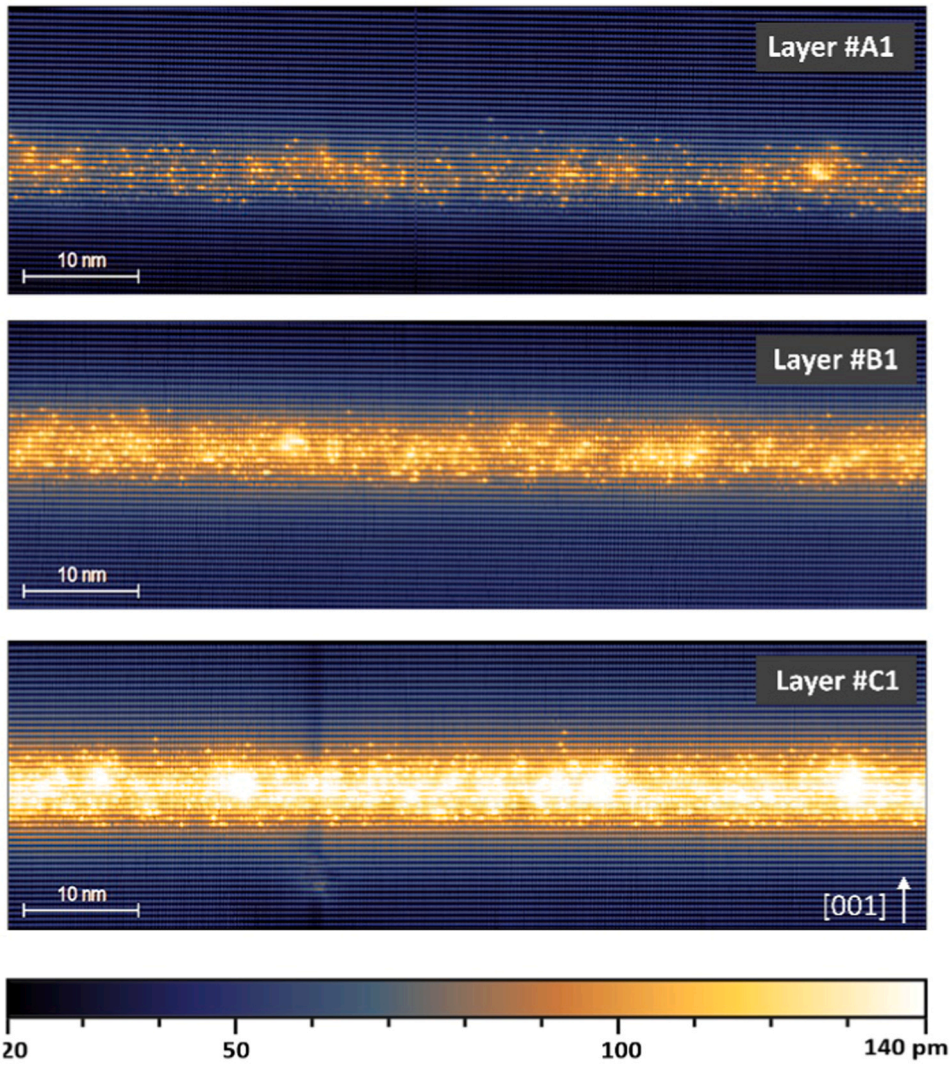

Fig. 2. Filled-state X-STM images (80×25 nm^2) of the SML-QDs layers A1 ((2×4), very low As flux), B1 (c(4×4), low As flux), and C1 (c(4×4), high As flux) from sample D with a bias voltage V_b = −2.1 V and a tunneling current I_t = 50 pA. The arrow indicates the growth direction [001].

3. Results

Fig. 2 shows atomically resolved topographic filled-state X-STM images of the SML-QDs layers A1, B1, and C1 from sample D. Although the structures of the three layers were nominally identical and all of them received exactly the same quantity of InAs material, one can see at least four striking differences in the X-STM measurements. First, since this kind of image provides real topographic information related to the local corrugation height above the cleaved surface due to the strain introduced by the In atoms (see color scale), it is clear that layer A1 contains much less In than the other layers, and that layer B1 contains slightly less In than layer C1. This is due to the fact that, under usual growth conditions, In incorporation is independent of the As flux (it is always unity), but, at lower As fluxes, it can be reduced below unity [23]. Since the As flux had to be considerably decreased to achieve a (2×4) reconstruction of the GaAs (001) surface, many In atoms deposited in layer A1 were not incorporated. Instead, they remained "floating" on the surface as adsorbed species (this effect is different from In segregation that will be discussed below) and were desorbed later when the substrate temperature was increased. Second, none of layers A1 to C1 show any vertical stacking of small 2D InAs islands. Rather, clusters of InGaAs material can be detected, mainly at higher As pressure (in layers B1 and C1), but there is clearly no periodicity inside them. This is most probably a consequence of the strong segregation effect of In atoms which is known to be present in the InAs/GaAs system where segregation coefficients R around 0.8 are often reported [23–27]. This very high value of R means that 80% of the In atoms that impinge on the surface will migrate to the next layer and will not be directly incorporated. This of course makes difficult to keep a high density of small 2D InAs islands, as most of them will be partially or even totally dissolved and their material will scatter around and form a background InGaAs layer, as can be seen in Fig. 2. Third, the density of these In-rich clusters increases with the As flux, reaching $1–2\times10^{10}$ cm^{-2}, $5–6\times10^{10}$ cm^{-2}, and $2–3\times10^{11}$ cm^{-2} in layers A1, B1, and C1, respectively. Fourth, a careful counting of the In atoms in empty-states X-STM images showed that In segregation decreases from layers A1 to C1, yielding values of R equal to 0.83 ± 0.02, 0.79 ± 0.01 and 0.72 ± 0.02, respectively, that are in excellent agreement with experimental data from in-situ RHEED measurements [28]. Considering that all the other parameters were kept fixed during the growth of these three layers of SML-QDs, this can only be a direct consequence of the variation of the As flux, as already previously observed [27].

We then studied how infrared photodetectors based on such SML-QDs behave as a function of the As flux. The spectral response of the SML-QDIP devices was measured at 12 K by Fourier transform infrared (FTIR) spectroscopy in normal incidence (with the radiation

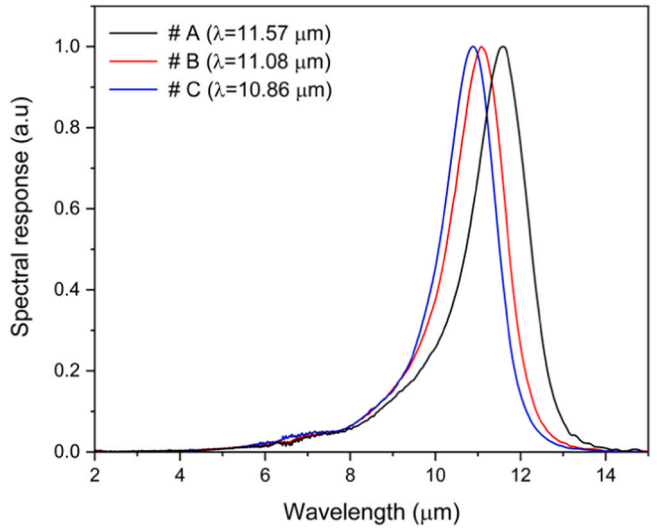

Fig. 3. Normalized spectral response of the SML-QDIPs obtained by FTIR in normal incidence at 12 K with a bias of + 1.1 V.

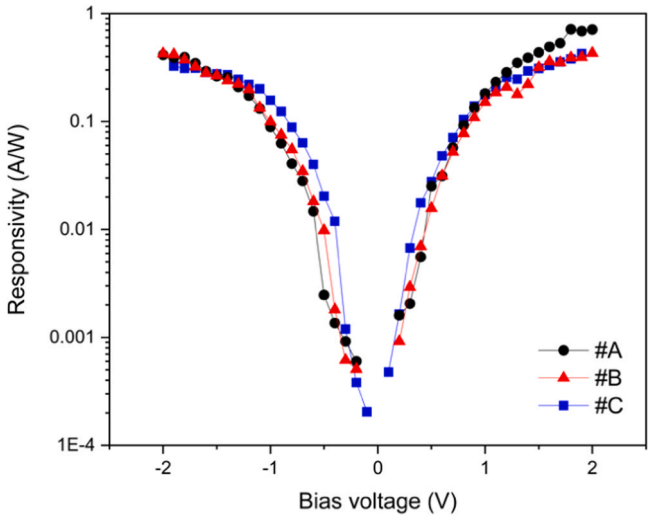

Fig. 4. Black-body responsivity of the three SML-QDIPs under normal incidence as a function of bias at 12 K.

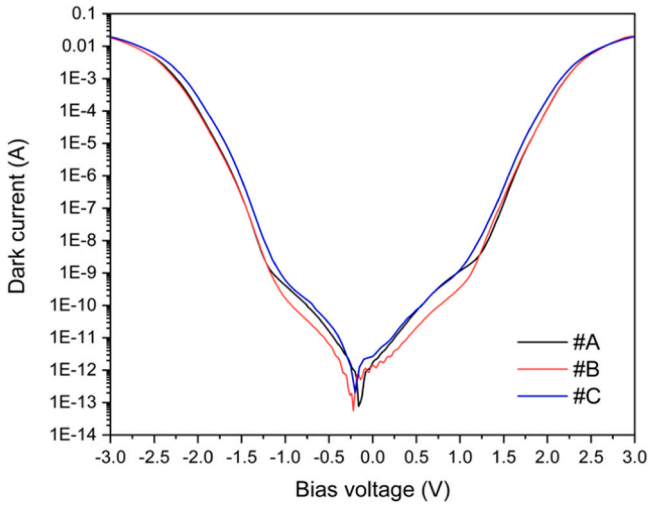

Fig. 5. Current versus voltage (I×V) curves in the dark (dark current) for SML-QDIPs A, B, and C obtained at 12 K using a dark+cold shield.

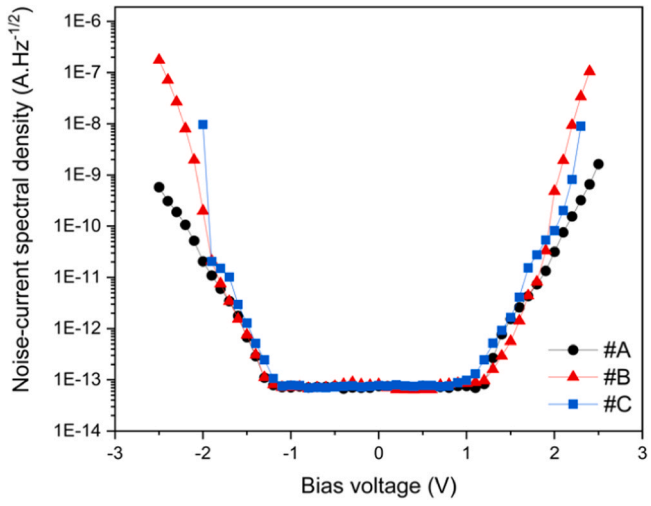

Fig. 6. Noise-current spectral density of SML-QDIPs A, B, and C as a function of bias voltage at 12 K with a dark+cold shield.

reaching the mesas from the top). Fig. 3 shows that the three spectra were very similar but systematically blue-shifted from QDIP A to C. Since $\Delta\lambda/\lambda$ is around 0.13 for all of them, it means that they involve a bound-to-bound transition. As the SML-QDs have a smaller size than conventional SK-QDs, they have a single confined state [29], and the peaks observed in Fig. 3 are due to an electronic transition from the ground state of the SML-QDs to the first (and only) excited state of the GaAs quantum well. The X-STM images show that increasing the As flux produces larger InGaAs nanostructures with higher In content. The combined effect is to reduce the energy of the SML-QD electron ground state relative to the excited state of the GaAs quantum well, producing the blueshift we observe in Fig. 3 as the As flux increases from sample A to C.

Responsivity measurements were used to determine the efficiency of the devices by taking the ratio of their electrical output (photocurrent generated in the mesas) to their optical input (power of the radiation falling on their optically active area). First, the spectral irradiance of a calibrated black body and total incident power were estimated. Then, the total photocurrent of the devices facing the calibrated black body (setup at 800 °C) was measured with lock-in techniques and allowed the calculation of the black-body responsivity reported in Fig. 4. One can see that the curves are very similar, showing a responsivity which monotonically increases up to a value around 0.6–0.8 A/W at a bias voltage of + 2 V.

The dark current of a photodetector is the electrical signal that can be measured between its two electrical contacts even without the presence of any external infrared radiation. Depending on its amplitude and temperature dependence, several properties of the devices can be inferred. These measurements were performed with a dark shield around the QDIPs that was also in thermal equilibrium with the sample holder. Fig. 5 shows the dark current of the three devices as a function of bias voltage. Once again, it can be observed that they have basically the same trends. Temperature dependent measurements revealed that the dark current was insensitive to temperature below 30 K and therefore was attributed to electronic tunneling through the $Al_{0.1}Ga_{0.9}As$ barriers [21]. Above 30 K, the dark current was thermally activated, as could be seen by its exponential temperature dependence that yielded an activation energy between 62 meV and 71 meV for SML-QDIPs A to C.

The intrinsic noise of the devices was also measured in the dark to minimize the absorption of any external radiation. Fig. 6 shows the noise current spectral density as a function of bias voltage. It was calculated by dividing the root-mean-square (RMS) noise current

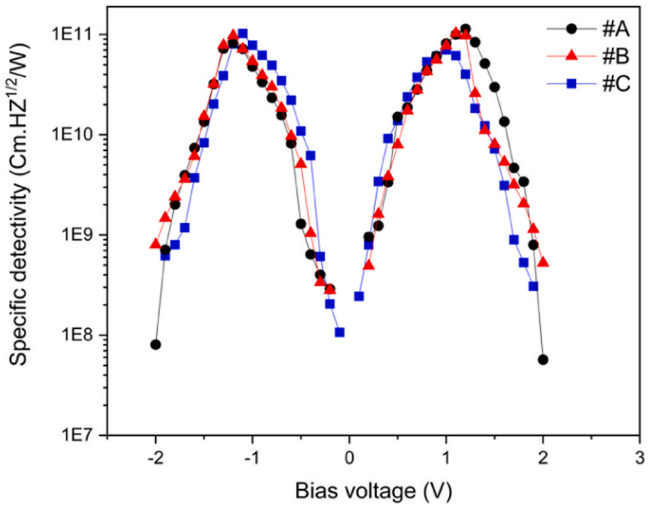

Fig. 7. Specific detectivity of SML-QDIPs A, B, and C as a function of bias voltage at 12 K.

coming from the devices by the square root of the bandwidth of the noise spectrum used by the spectrum analyzer in order to get a noise value that is independent of the experimental parameters. In photoconductive photodetectors, the main source of intrinsic noise usually comes from the generation-recombination (g-r) processes associated with the dark current which is often several orders of magnitude larger than the photocurrent itself. One therefore expects the noise curves to show the same features as the dark current. This is the case in Fig. 6 where the plateau observed at low bias voltage is due to the limitation of the experimental setup to measure a signal below its intrinsic background-noise level of 7×10^{-14} A $Hz^{-1/2}$.

The specific detectivity D^* (signal to noise ratio) of all three SML-QDIPs was calculated as a function of bias voltage at 12 K and is reported in Fig. 7. The objective of D* as a figure of merit is to provide a way to compare devices of different nature and size measured in different experimental conditions. Its value is defined as $D^* = R\sqrt{A}/i_n$, where R is the black-body responsivity, A is the optically active area of the mesas, and i_n is the noise-current spectral density. Although the responsivity increases monotonically up to ± 2 V, the specific detectivity has a maximum around ± 1.1 V as a consequence of the strong increase of the noise beyond this bias voltage. The maximum specific detectivities of 1.13×10^{11} cm $Hz^{1/2}$ W^{-1}, 1.03×10^{11} cm $Hz^{1/2}$ W^{-1}, and 1.03×10^{11} cm $Hz^{1/2}$ W^{-1} were achieved in SML-QDIPs A, B, and C, respectively.

4. Discussion

When the main figures of merit of the three SML-QDIPs are compared, the only significant difference is the blueshift of the spectral response when the As flux rises from SML-QDIP A–grown with a very low As flux to achieve the (2×4) surface reconstruction–to SML-QDIP C that has the highest As flux generally used for the growth of conventional InAs SK-QDs. The similarities between the other properties, though, contrast with the striking differences revealed in the X-STM images of Fig. 2. Therefore, the first thing that one might wonder is whether the absorption signal reported in Fig. 3 really comes from the In-rich clusters that are observed in the X-STM images. Could this signal instead come from the diluted InGaAs quantum well that forms around the SML-QDs as a consequence of the strong segregation of the In atoms present in all three samples? This argument is supported by the fact that the photoluminescence (PL) spectrum of SML-QDs is generally much narrower than that of SK-QDs and is similar to that of an InGaAs QW with the same thickness and average In content [29]. However, the answer is very simple: there is no way that such a strong detectivity in the 10^{11} cm $Hz^{1/2}$/W range can be attributed to InGaAs QWs. All the measurements reported in Figs. 3–7 were performed in normal incidence, and it is well known that, in such conditions, intersubband transitions are prohibited in 2D systems due to polarization rules [30]. This is why QWIPs always need an extra diffraction grating (or any other equivalent mechanism) on top of the devices to operate properly in normal incidence. As a result, the strong signal measured in our SML-QDIPs–these devices have among the highest detectivity values reported to date [17,31]–can only be due to the 3D confinement of carriers inside the In-rich clusters observed in the X-STM images, and the blueshift of the spectral response must be related to the size variation of these clusters that behave as quantum dots [32].

One might therefore question why the performance of these three devices is so similar if the density of SML-QDs increases roughly by a factor of ten from device A to device C. The answer seems to be related to the fact that SML-QDs are smaller than usual SK-QDs, have a much lower In concentration and, consequently, contain only a single confined electronic state (their ground state). The energy of this state is so close to the top of the potential barrier that the wave function of the confined electrons is only weakly localized. Since SML-QDs can reach extremely high areal densities (up to 10^{12} cm^{-2} [13]), their lateral separation can be very small (just a few nm), allowing their ground-state wave function to overlap the closest nanostructures [29]. As a result, due to the Pauli Exclusion Principle, when an electron is confined in a specific SML-QD, the closest nanostructures will have a low probability to be populated, limiting thus the optical activity (and device performance) of samples having the highest densities of SML-QDs. Although the holes (that have a heavier effective mass) are confined in individual SML-QDs, the optical properties of the system are governed by the lighter electrons, and the Bohr radius of the exciton is therefore much larger than the size of a single SML-QD, promoting an averaging of the local composition fluctuations inside the dilute InGaAs quantum well. This results, for instance, in a narrower PL spectrum, compared with SK-QDs [13], despite the fact that SML-QDs are clearly more inhomogeneous in size, in contrast to what is often claimed in the literature [29].

Since the experimental results of the three SML-QDIPs look so similar, one might wonder as well if it is worth the effort to grow SML-QDs on the (2×4) surface reconstruction, as in SML-QDIP A. These growth conditions are more difficult to adjust and the growth time for this device is also much longer, resulting from the lower deposition rates that must be used as a consequence of the low As flux required to achieve that surface reconstruction. If both types of SML-QDs were already fully optimized, the obvious answer would be no, as the easier growth conditions used for SK-QDs might also be used to grow SML-QDs with excellent results (superior to the ones of SK-QDs [15,17]), as shown by SML-QDIP C. However, it is very clear from Fig. 2 that the current growth conditions are probably far from being optimized. Indeed, as can be seen in the X-STM images, none of the clusters detected in the layers have the full 18 MLs height expected from the nominal structure. In addition, none of them showed any vertical stacking of small 2D InAs islands pictured in Fig. 1. Although such features are not expected for layers grown with a c(4×4) reconstruction, which favors a random incorporation of the In atoms [18], there is hope that, after further optimization of the growth conditions, taller nanostructures showing vertical stacking might occur in the presence of a (2×4) surface reconstruction [19], leading to better SML-QDs and QDIPs.

Both the smaller height of the QDs and the absence of stacked 2D islands are clearly a consequence of the strong In segregation that promotes the migration of most In atoms toward the surface [23]. These In atoms will incorporate later but not necessarily into the stacks of 2D islands (if any), leading to the formation of the 18 ML-

thick dilute InGaAs layer surrounding the SML-QDs. This decreases the In content of the SML-QDs and reduces the internal strain field that was supposed to align the small 2D InAs islands of the next SML cycles. As a matter of fact, one expects the 2D InAs islands of a SML-QD to vertically align in the same way SK-QDs do in consecutive InAs layers when their separation is small. Xie et al. [33] provided a semi-empirical model able to explain this effect based on mechanochemical properties of the diffusion of In adatoms on a GaAs surface. They introduced a parameter z_0 defining the thickness of the GaAs spacer below which the alignment of SK-QDs belonging to two consecutive InAs layers always occurs:

$$z_0 = r_0\left(\frac{8}{l}\frac{L_D}{k_B}\frac{X}{T}\right)^{\frac{1}{3}} \quad (1)$$

where r_0 is the radius of a sphere having the same volume as the SK-QDs, L_D is the diffusion length of the In adatoms, l is the average lateral distance between SK-QDs within the same InAs layer, k_B is the Boltzmann constant, and T is the absolute temperature of the growth process. X is a factor that takes account of the elastic properties of both materials and of the strain present in the InAs/GaAs system, being defined as

$$X = \frac{3}{3B_{InAs}+2}\frac{B_{InAs}}{Y_{GaAs}/(1+\gamma_{GaAs})}\quad\frac{V_{InAs}}{2}\frac{}{Y_{InAs}}\quad (C_{11}^{InAs}\quad \varepsilon_0)^2 \quad (2)$$

where B_{InAs} and Y_{InAs} are the bulk modulus and Young´s modulus of InAs, Y_{GaAs} and γ_{GaAs} are Young´s modulus and Poisson´s ratio of GaAs, V_{InAs} and C_{11}^{InAs} are the unstrained atomic volume and elastic constant of InAs, and ε_0 is the elastic strain of the InAs/GaAs system due to the lattice mismatch.

For InAs SK-QDs having a pyramidal shape (base = 170 Å and height = 35 Å) and an areal density of 3.5×10^{10} cm^{-2}, Xie et al. estimated that all QDs from consecutive InAs layers could be fully aligned whenever the GaAs spacer was thinner than 35.6 MLs (~100 Å), and were totally uncorrelated for spacers thicker than 200 MLs (~565 Å). These results were in excellent agreement with their experimental data, and Eqs. (1 and 2) were successfully used to provide the first value (z_0 =35.6 MLs) taking r_0= 37 Å, L_D= 0.28 µm, l= 535 Å, and adopting typical values from the literature for the elastic properties and lattice constants of InAs and GaAs.

Due to the very thin GaAs spacer used between consecutive InAs submonolayers, literature usually assumes that such a vertical alignment also happens inside SML-QDs, and this is why they are always sketched as stacks of narrow 2D InAs islands separated by thin layers of GaAs material. However, one should be aware of several relevant differences with respect to the case of SK-QDs. 1) The SML deposition technique provides (when successful) only small 2D InAs islands that are around 5 nm wide, yielding a much smaller value of r_0 (~11 Å) than for usual InAs SK-QDs that are much wider and higher. 2) The density of SML-QDs may be around 10 times higher than that of SK-QDs, leading to a lateral distance between SML-QDs three times smaller. 3) The In diffusion length L_D is much smaller for SML-QDs due to the presence of strong In segregation. Indeed, for very thin GaAs spacers, the quantity of In atoms adsorbed at the surface can be very high, and this large population of adatoms considerably reduces their mobility. For instance, considering a typical segregation coefficient of 0.8 and the case of our SML-QDs consisting of 6 repetitions of 0.5 ML of InAs followed by 2.5 MLs of GaAs, the population of In adatoms at the GaAs surface after the first cycle is equivalent to a coverage of 0.26 ML, and it keeps increasing after each cycle up to a coverage of 0.52 ML after the sixth cycle [28]. This excess of In adatoms at the GaAs surface just before InAs deposition doesn´t happen during the growth of consecutive layers of SK-QDs, where the GaAs spacers are much thicker, because, for such values of R, the manifestations of In segregation are no longer relevant after 20 MLs of GaAs [34]. 4) Another important consequence of segregation is that the original 2D InAs islands that were eventually nucleated at the surface will lose most of their In atoms during capping and will no longer be made of pure InAs material. The In atoms that escaped and segregated with the growth front will be randomly incorporated later, forming the wide and dilute InGaAs QW around the SML-QDs. Thus, the surrounding matrix and thin spacer layer between each InAs submonolayer no longer consist of GaAs material neither. Since the original InAs/GaAs system sketched in Fig. 1 is replaced by In rich islands scattered in a dilute InGaAs QW, the local strain ε_0 becomes much lower, all the elastic constants of both materials are now more alike, and the final value of z_0 can drop below 2 MLs, confirming that an effective stacking of the 2D islands no longer occurs. Although this semi empirical model might not be fully suited to simulate the strain field around 2D InAs islands, it clearly points out that the strain in such a system is much lower than for SK-QDs, as can be clearly observed in the X-STM images that don´t show any evidence of stacked 2D islands.

Since the literature invariably reports SML-QDs studies involving growth conditions similar to the ones of SK-QDs, and our present results strongly suggest that further optimization is required to take advantage of the full potential of such nanostructures, one should definitely seek alternative ways to improve their growth. Considering that segregation is a thermally activated process, an easy way to reduce its strength and prevent In atoms from escaping from the 2D InAs islands would be to lower the sample temperature during deposition of the InAs/GaAs cycles. As the activation energy of this phenomenon is quite small (0.11–0.12 eV) [24,35], reducing the sample temperature to 350 °C would only decrease the segregation coefficient down to around 0.5. Although previous studies have shown that such a low temperature is enough to cancel the influence of segregation on some optical and structural properties [23,34], it is clearly not enough to eliminate the phenomenon itself. Nevertheless, the SML-QDs would likely have a higher In content and a stronger internal strain field. That would lead to better alignment of the 2D InAs islands and to taller InGaAs nanostructures (hopefully with their full expected height) showing a stronger carrier confinement. Of course, a reduction of the sample temperature would also be accompanied by an increase of the density of structural defects. Yet, such point defects–mainly antisites [36]–would be restricted to the 18 MLs of the SML-QDs and most of them would probably disappear later during deposition of the next layers at higher growth temperature that would provide a thermal annealing.

The other problem highlighted by the X-STM image of layer A1 (Fig. 2) was the strong reduction of In incorporation related to the low As flux used to achieve the (2×4) surface reconstruction. To deal with this issue, one actually should go in the opposite direction. Indeed, InAs QDs are often deposited at 515–490 °C to minimize In desorption from the surface. When the sample temperature is lowered from 570 °C–necessary to grow good-quality GaAs material–to 515–490 °C, the surface morphology undergoes a change around 520 °C, switching from a (2×4) reconstruction at high temperature to a c(4×4) reconstruction at low temperature. To recover the (2×4) reconstruction needed to allow the nucleation of true 2D InAs island on the surface [19], the As flux has to be considerably decreased [20] (around a factor of 10), and it is this strong reduction of the flux that limits In incorporation observed in layer A1 of Fig. 2. One way to avoid this problem would be to keep the sample temperature slightly above 520 °C in order to maintain the original (2×4) reconstruction in the presence of a high As flux. The In-desorption rate will not be significantly higher than usual but, in any case, small increases can easily be taken into account by calibrating the exact InAs growth rate at that temperature. Segregation will also be slightly higher, thus increasing the escape rate of the In atoms from the InAs islands, but this approach would provide an effective way to confirm which of both strategies–segregation control or use of a (2×4) surface reconstruction–has a larger impact on the formation of SML-QDs and on the performance of their infrared photodetectors.

5. Conclusion

The electro-optical properties of three infrared photodetectors based on InAs/GaAs submonolayer quantum dots grown with a different arsenic flux revealed very similar figures of merit and an excellent specific detectivity in the 10^{11} cm $Hz^{1/2}$ W^{-1} range. This is in contrast with the results of cross-sectional scanning tunneling microscopy which showed that SML-QDs growth is highly sensitive to the As flux. For the lowest arsenic flux that yielded a (2×4) reconstruction of the GaAs(001) surface, the density of InGaAs nanostructures was considerably reduced, and a lower incorporation and enhanced segregation of In atoms were detected. Higher values of the As flux always led to a c(4×4) reconstruction with higher In incorporation and density of quantum dots. These nanostructures did not develop to their full expected height and did not consist of stacks of small two-dimensional InAs islands. In fact, the X-STM data revealed that the submonolayer quantum dots were actually In-rich clusters embedded in a wider dilute InGaAs quantum well. Such features result from the strong segregation of In atoms that is typical in the strained InAs/GaAs system. It leads to the migration of around 80% of the In atoms from one atomic layer to the next one, inhibiting the formation of true 2D InAs islands and their vertical stacking that would be necessary to obtain typical submonolayer quantum dots. The lack of In in the nanostructures reduces their internal strain and size, and increases the bandgap of their material, leading to shallower energy levels and electronic wave functions that extend over the closest clusters, weakening thus their overall 3D confinement and the advantage of samples having a high density of nanostructures. As a consequence, one way to deal with these problems is to reduce In segregation, which can usually be done by simply decreasing the growth temperature. However, if one wants to keep the (2×4) surface reconstruction needed to provide true 2D InAs islands, lower temperatures imply an even lower As flux which in turn results in a weaker In incorporation. Therefore, an alternative way to improve the growth quality and performance of SML-QDs devices might be to grow the nanostructures at slightly higher temperature and with a much higher As flux in order to keep the surface reconstruction of the GaAs(001) surface just above the (2×4) to c(4×4) transition.

CRediT authorship contribution statement

A. Alzeidan: Investigation, Validation, Formal analysis, Data curation, Writing – original draft, Visualization. **T. F. Cantalice:** Investigation, Software. **K. D. Vallejo:** Investigation. **R.S.R. Gajjela:** Investigation, Validation, Formal analysis, Data curation. **A. L. Hendriks:** Validation, Formal analysis. **P. J. Simmonds:** Resources, Supervision, Writing – review & editing, Funding acquisition. **P.M. Koenraad:** Resources, Supervision, Writing – review & editing, Funding acquisition. **A. A. Quivy:** Conceptualization, Methodology, Writing – review & editing, Supervision, Funding acquisition, Project administration.

Declaration of Competing Interest

The authors declare that they have no known competing financial interests or personal relationships that could have appeared to influence the work reported in this paper.

Acknowledgements

This study was financed in part by the Coordenação de Aperfeiçoamento de Pessoal de Nível Superior - Brasil (CAPES) - Finance Code 001, by CNPq (grant 311687/2017-2), and by European Union's Horizon 2020 research and innovation program under the Marie Skłodowska-Curie project 4PHOTON grant agreement No 721394.

References

[1] V. Ryzhii, I. Khmyrova, M. Ryzhii, V. Mitin, Comparison of dark current responsivity and detectivity in different intersubband infrared photodetectors, Semicond. Sci. Technol. 19 (2003) 8–16, https://doi.org/10.1088/0268-1242/19/1/002
[2] S. Krishna, Quantum dots-in-a-well infrared photodetectors, J. Phys. D. 38 (2005) 2142–2150, https://doi.org/10.1088/0022-3727/38/13/010
[3] J. Phillips, Evaluation of the fundamental properties of quantum dot infrared detectors, J. Appl. Phys. 91 (2002) 4590–4594, https://doi.org/10.1063/1.1455130
[4] P. Martyniuk, S. Krishna, A. Rogalski, Assessment of quantum dot infrared photodetectors for high temperature operation, J. Appl. Phys. 104 (2008) 034314, https://doi.org/10.1063/1.2968128
[5] S. Tsao, H. Lim, W. Zhang, M. Razeghi, High operating temperature 320 × 256 middle-wavelength infrared focal plane array imaging based on an InAs/ InGaAs/ InAlAs/ InP quantum dot infrared photodetector, Appl. Phys. Lett. 90 (2007) 201109, https://doi.org/10.1063/1.2740111
[6] A.D. Stiff, S. Krishna, P. Bhattacharya, S. Kennerly, High-detectivity normal-incidence mid-infrared (λ~4 μm) InAs/GaAs quantum-dot detector operating at 150 K, Appl. Phys. Lett. 79 (2001) 421–423, https://doi.org/10.1063/1.1385584
[7] P.B. Joyce, T.J. Krzyzewski, G.R. Bell, B.A. Joyce, T.S. Jones, Composition of InAs quantum dots on GaAs(001): direct evidence for (In,Ga)As alloying, Phys. Rev. B. 58 (1998) R15981–R15984, https://doi.org/10.1103/PhysRevB.5 8.R15981
[8] F. Patella, M. Fanfoni, F. Arciprete, S. Nufris, E. Placidi, A. Balzarotti, Kinetic aspects of the morphology of self-assembled InAs quantum dots on GaAs(001), Appl. Phys. Lett. 78 (2001) 320–322, https://doi.org/10.1063/1.1339850
[9] J.X. Chen, A. Markus, A. Fiore, U. Oesterle, R.P. Stanley, J.F. Carlin, R. Houdré, M. Ilegems, L. Lazzarini, L. Nasi, M.T. Todaro, E. Piscopiello, R. Cingolani, M. Catalano, J. Katcki, J. Ratajczak, Tuning InAs/GaAs quantum dot properties under stranski-krastanov growth mode for 1.3μm applications, J. Appl. Phys. 91 (2002) 6710–6716, https://doi.org/10.1063/1.1476069
[10] M.J. da Silva, A.A. Quivy, P.P. Gonzalez-Borrero, N.T. Moshegov, E. Marega Jr., Correlation between structural and optical properties of InAs quantum dots along their evolution, J. Cryst. Growth 227–228 (2001) 1025–1028, https://doi.org/10.1016/S0022-0248(01)00981-2
[11] M.J. da Silva, A.A. Quivy, S. Martini, T.E. Lamas, E.C.F. da Silva, J.R. Leite, Large InAs/GaAs quantum dots with an optical response in the long-wavelength region, J. Cryst. Growth 278 (2005) 103–107, https://doi.org/10.1016/j.jcrysgro.2004.12.118
[12] I.L. Krestnikov, N.N. Ledentsov, A. Hoffmann, D. Bimberg, Arrays of two-dimensional islands formed by submonolayer insertions: growth, properties, devices, Phys. Stat. Solidi (a) 183 No. 2 (2001) 207–233, https://doi.org/10.1002/1521-396X(200102)183:2<207::AID-PSSA207>3.0.CO;2-2
[13] Andrea Lenz, Holger Eisele, Jonas Becker, Jan-Hindrik Schulze, Tim D. Germann, Franziska Luckert, Konstantin Pötschke, Ernst Lenz, Lena Ivanova, André Strittmatter, Dieter Bimberg, Udo W. Pohl, Mario Dähne, Atomic structure and optical properties of InAs submonolayer depositionsin GaAs, J. Vaccum Sci. Technol. B 29 (2011) 04D104, https://doi.org/10.1116/1.3602470
[14] David Z.-Y. Ting, Sumith V. Bandara, Sarath D. Gunapala, Jason M. Mumolo, Sam A. Keo, Cory J. Hill, John K. Liu, Edward R. Blazejewski, Sir B. Rafol, Yia-Chung Chang, Submonolayer quantum dot infrared photodetector, Appl. Phys. Lett. 94 (2009) 111107, https://doi.org/10.1063/1.3095812
[15] S. Sengupta, J.O. Kim, A.V. Barve, S. Adhikary, Y.D. Sharma, N. Gautam, S.J. Lee, S.K. Noh, S. Chakrabarti, S. Krishna, Sub-monolayer quantum dots in confinement enhanced dots-in-a-well heterostructure, Appl. Phys. Lett. 100 (2012) 191111, https://doi.org/10.1063/1.4711214
[16] David Z.-Y. Ting, Yia-Chung Chang, Sir B. Rafol, John K. Liu, Cory J. Hill, Sam A. Keo, Jason Mumolo, Sarath D. Gunapala, Sumith V. Bandara, The sub-monolayer quantum dot infrared photodetector revisited, Infrared Phys. Technol. 70 (2015) 20–24, https://doi.org/10.1016/j.infrared.2014.09.028
[17] H. Ghadi, S. Sengupta, S. Shetty, A. Manohar, A. Balgarkashi, S. Chakrabarti, N.B. Pendyala, S.L. Prajapati, A. Kumar, Comparison of three design architectures for quantum dot infrared photodetectors: InGaAs-capped dots, dots-in-a-well, and submonolayer quantum dots, IEEE Trans. Nanotechnol. 14 (2015) 603, https://doi.org/10.1109/TNANO.2015.2432044
[18] J.G. Belk, C.F. McConville, J.L. Sudijono, T.S. Jones, B.A. Joyce, Surface alloying at InAs-GaAs interfaces grown on (001) surfaces by molecular beam epitaxy, Surf. Sci. 387 (1997) 213–226, https://doi.org/10.1016/S0039-6028(97)00355-5
[19] G.R. Bell, T.J. Krzyzewski, P.B. Joyce, T.S. Jones, Island size scaling for submonolayer growth of InAs on GaAs(001)-(2×4): strain and surface reconstruction effects, Phys. Rev. B 61 (2000) R10551–R10554, https://doi.org/10.1103/PhysRevB.61.R10551
[20] Vincent P. LaBella, Michael R. Krause, Zhao Ding, Paul M. Thibado, Arsenic-rich GaAs(001) surface structure, Surf. Sci. Rep. 60 (2005) 1–53, https://doi.org/10.1016/j.surfrep.2005.10.001
[21] A. Alzeidan, M.S. Claro, A.A. Quivy, High-detectivity infrared photodetector based on InAs submonolayer quantum dots grown on GaAs(001) with a 2 × 4 surface reconstruction, J. Appl. Phys. 126 (2019) 224506, https://doi.org/10.1063/1.5125238
[22] R.S.R. Gajjela, A.L. Hendriks, A. Alzeidan, T.F. Cantalice, A.A. Quivy, P.M. Koenraad, Cross-sectional scanning tunneling microscopy of InAs/GaAs(001) submonolayer

quantum dots, Phys. Rev. Mater. 4 (2020) 114601, https://doi.org/10.1103/PhysRevMaterials.4.114601
[23] K. Muraki, S. Fukatsu, Y. Shiraki, R. Ito, Surface segregation of In atoms during molecular beam epitaxy and its influence on the energy levels in InGaAs/GaAs quantum wells, Appl. Phys. Lett. 61 (1992) 557–559, https://doi.org/10.1063/1.107835
[24] S. Martini, A.A. Quivy, E.C.F. da Silva, J.R. Leite, Real-time determination of the segregation strength of indium atoms in InGaAs layers grown by molecular-beam epitaxy, Appl. Phys. Lett. 81 (2002) 2863–2865, https://doi.org/10.1063/1.1513182
[25] J.G. Keizer, A.B. Henriques, A.D.B. Maia, A.A. Quivy, P.M. Koenraad, Atomically resolved study of the morphology change of InAs/GaAs quantum dot layers induced by rapid thermal annealing, Appl. Phys. Lett. 101 (2012) 243113, https://doi.org/10.1063/1.4770371
[26] S. Martini, A.A. Quivy, T.E. Lamas, E.C.F. da Silva, Real-time RHEED investigation of indium segregation in InGaAs layers grown on vicinal GaAs(001) substrates, Phys. Rev. B 72 (2005) 153304, https://doi.org/10.1103/PhysRevB.72.153304
[27] S. Martini, A.A. Quivy, T.E. Lamas, M.J. da Silva, E.C.F. da Silva, J.R. Leite, Influence of indium segregation on the RHEED oscillations during the growth of InGaAs layers on a GaAs(001) surface, J. Cryst. Growth 251 (2003) 101–105, https://doi.org/10.1016/S0022-0248(02)02313-8
[28] T.F. Cantalice, A. Alzeidan, S.M. Urahata, A.A. Quivy, In-situ measurement of Indium segregation in InAs/GaAs submonolayer quantum dots, Mater. Res. Express 6 (1–10) (2019) 126205, https://doi.org/10.1088/2053-1591/ab55a8
[29] S. Harrison, M.P. Young, P.D. Hodgson, R.J. Young, M. Hayne, L. Danos, A. Schliwa, A. Strittmatter, A. Lenz, H. Eisele, U.W. Pohl, D. Bimberg, Heterodimensional charge-carrier confinement in stacked submonolayer InAs in GaAs, Phys. Rev. B 93 (2016) 085302, https://doi.org/10.1103/PhysRevB.93.085302
[30] B.F. Levine, Quantum well infrared photodetectors, J. Appl. Phys. 74 (1993) R1–R81, https://doi.org/10.1063/1.354252
[31] J.O. Kim, S. Sengupta, A.V. Barve, Y.D. Sharma, S. Adhikary, S.J. Lee, S.K. Noh, M.S. Allen, J.W. Allen, S. Chakrabarti, S. Krishna, Multi-stack InAs/InGaAs submonolayer quantum dots infrared photodetectors, Appl. Phys. Lett. 102 (2013) 011131, https://doi.org/10.1063/1.4774383
[32] S. Unsleber, M. Deppisch, C.M. Krammel, M. Vo, C.D. Yerino, P.J. Simmonds, M. Larry Lee, P.M. Koenraad, C. Schneider, S. Höfling, Bulk AlInAs on InP(111) as a novel material system for pure single photon emission, Opt. Express 24 (2016) 23198, https://doi.org/10.1364/OE.24.023198
[33] Qianghua Xie, Anupam Madhukar, Ping Chen, Nobuhiko P. Kobayashi, Vertically self-organized inas quantum box islands on GaAs(100), Phys. Rev. Lett. 75 (1995) 2542–2545, https://doi.org/10.1103/PhysRevLett.75.2542
[34] S. Martini, A.A. Quivy, M.J. da Silva, T.E. Lamas, E.C.F. da Silva, J.R. Leite, E. Abramof, Ex-situ investigation of indium segregation in InGaAs/GaAs quantum wells using high-resolution x-ray diffraction, J. Appl. Phys. 94 (2003) 7050–7052, https://doi.org/10.1063/1.1621738
[35] R. Kaspi, K.R. Evans, Improved compositional abruptness at the InGaAs on GaAs interface by presaturation with In during molecular-beam epitaxy, Appl. Phys. Lett. 67 (1995) 819–821, https://doi.org/10.1063/1.115454
[36] S. Fleischer, C.D. Beling, S. Fung, W.R. Nieveen, J.E. Squire, J.Q. Zheng, M. Missous, Structural and defect characterization of GaAs and $Al_xGa_{1-x}As$ grown at low temperature by molecular beam epitaxy, J. Appl. Phys. 81 (1997) 190–198, https://doi.org/10.1063/1.364105

A. Alzeidan obtained a Bachelor of Science degree in Physics from University of Damascus (Syria) in 2011, and a Master´s degree in Physics from the University of São Paulo (Brazil) in 2017, where he is currently a Ph.D. student (last year). His work is related to the molecular-beam epitaxy of infrared photodetectors based on In(Ga)As submonolayer quantum dots, and on their processing and opto-electrical characterization.

T. Cantalice obtained a Bachelor of Science degree in Physics from the University of São Paulo (Brazil) in 2012, and a Master´s degree in Physics from the State University of Campinas (Brazil) in 2015. Since 2017, he is a Ph.D. student at the University of São Paulo, and his work is related to the investigation of Indium segregation in infrared photodetectors based on In(Ga)As quantum dots. He is also currently working as a Data Scientist for a Brazilian health company.

Kevin Vallejo is a Ph.D. student at Boise State University scheduled to graduate in the Fall of 2021. He obtained a Bachelor of Science degree from The University of Texas at El Paso in 2016, and a Master´s degree in Engineering from Boise State University in 2020. During the Spring 2015 semester, Kevin received the US Department of State Benjamin A. Gilman scholarship to study at Åbo Akademi University in Finland. In 2019, he received the US National Nuclear Science Foundation Graduate Fellowship, the US Intelligence Community Postdoctoral Fellowship, and Dean's Scholar award from Boise State University for outstanding scholarship.

Raja S. R. Gajjela is currently an Early Stage Researcher (Marie Skłodowska-Curie Actions) at the Eindhoven University of Technology, The Netherlands, since 2019 working on the cross-sectional scanning tunneling microscopy of self-assembled III-V semiconductor quantum dots. He got his M.Sc. degree in Materials Engineering and Nanotechnology from Politecnico Di Milano, Italy in 2018 with the thesis on MOVPE growth of Sb_2Te_3 thin films and nanowire arrays at the National Research Council of Italy - Institute for Microelectronics and Microsystems (CNR-IMM), Milan, Italy. He graduated (2016) with a gold medal for Bachelor's in Metallurgy and Material Technology, Yogi Vemana University, India.

Arthur L. Hendriks graduated from Eindhoven University of Technology in 2020 with a Master's degree in Physics. He did this work in the Photonics and Semiconductor Nanophysics (PSN) subgroup of Paul Koenraad. During his master thesis, he used cross-sectional scanning tunneling microscopy (X-STM) to measure high density quantum dot structures. Currently, he is a Ph.D. student in the PSN subgroup of Andrea Fiore. In his project, he fabricates and optimizes fiber-tip sensors consisting of photonic crystal structures on the cleaved facet of a fiber.

Dr. Paul Simmonds completed his Ph.D. in semiconductor physics at the University of Cambridge in 2008, followed by postdoctoral positions at the University of Minnesota, UCSB, and Yale University. Starting in 2011, he managed the Integrated NanoMaterials Laboratory at UCLA, and Chaired the IEEE Photonics Society chapter. Dr. Simmonds joined Boise State University in 2014, with joint appointments in Physics and Materials Science, and was promoted to Associate Professor in 2020. He is a Senior Member of the IEEE, winner of the 2018 North American Molecular Beam Epitaxy Young Investigator award, and a US National Science Foundation CAREER awardee.

Paul Koenraad graduated from Utrecht University in 1986 with a master's degree in physics and defended his thesis in the Department of Applied Physics at Eindhoven University of Technology in 1990. He continued his career in Eindhoven where he is now full professor since 2003. He has worked as visiting scientist at IBM Zurich, University of São Paulo, and the University of New South Wales in Sydney. His research interest is focused on III-V semiconductor nanostructures and dopants, and he is an Internationally leading expert on the application of scanning probe techniques to semiconductor nanostructures and impurities in semiconductors.

A. A. Quivy graduated in 1986 and got his Master´s degree (1986) and Ph.D. (1991) in Physics from Université Libre de Bruxelles (Belgium). He is a Professor of Physics at Universidade de São Paulo (Brazil) since 1992, was a visiting scientist at Center for Quantum Devices (Northwestern University, USA) in 2005 and 2006, and is an Associate Professor since 2012. His main research topics are molecular beam epitaxy and morphological, structural, and opto-electrical characterization of III–V compounds. Lately, he has been investigating the growth, processing and testing of III–V solar cells and infrared photodetectors based on quantum dots.